



Research article

Adsorption of sulfur on Lanxess Lewatit® AF 5 resin during the acidic albion leaching process for chalcopyrite

Omid Marzoughi^{*}, Chris Pickles, Ahmad Ghahreman

Robert M. Buchan Department of Mining, Queen's University, Kingston, ON K7L 3N6, Canada



ARTICLE INFO

Keywords:

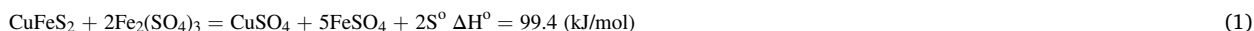
Acidic albion leaching
Chalcopyrite
Lanxess Lewatit® AF 5
Adsorption
Adsorption isotherm
Elemental sulfur

ABSTRACT

Elemental sulfur is one of the major byproducts of the acidic Albion leaching process for chalcopyrite. It is a challenging component in the leach solution as it impedes gold recovery from the residue. Lanxess Lewatit® AF 5 (AF 5) is a microporous carbon-based resin, which is being investigated for the removal of elemental sulfur during this leaching process. In the current research, a series of leaching experiments were performed as a function of temperature, agitation speed and concentrate to AF 5 ratio. Using these results, the adsorption isotherms, the kinetics and the thermodynamics of sulfur removal were studied. One hundred percent of the elemental sulfur could be adsorbed by the AF 5 resin from the acidic Albion leaching process for chalcopyrite. Adsorption isotherms at various temperatures were determined using the Langmuir and Freundlich models. The maximum sorption capacity of AF 5 at 95 °C was 488 mg/g. The kinetic data were fitted to pseudo-first order (PFO) and pseudo-second order (PSO) models and it was shown that the PFO model was best suited to describe the results. The rapid kinetics of sulfur adsorption were attributed to the open pore structure of the AF 5. The Gibbs free energy, enthalpy and entropy of sulfur adsorption by AF 5 were determined as follows: $\Delta G_{\text{ads}}^{\circ} = -1.9$ kJ/mol, $\Delta H_{\text{ads}}^{\circ} = -9.1$ kJ/mol, and $\Delta S_{\text{ads}}^{\circ} = -0.1$ kJ/(mol K). The negative free energy and enthalpy changes demonstrated that the adsorption of elemental sulfur was both spontaneous and exothermic over the temperature range studied.

1. Introduction

The acidic Albion leaching process for chalcopyrite, is an example of an oxidative leaching process for sulfide minerals, where copper and iron are recovered. However, elemental sulfur is generated as a by-product and this sulfur can have negative impacts on both the leaching process and also downstream processing [1,2,3,4,5,6]. The chalcopyrite leaching reaction can be described as follows [2,3]:



In this reaction the sulphide sulfur is oxidised to elemental sulfur. The reaction is initially rapid but then begins to slow down. This reaction produces elemental sulfur, which accumulates on the mineral surface, and could act as a diffusion barrier to the transport of reagent products between the leaching solution and the mineral surface. Evidence of an impervious sulfur layer has been obtained by observation and characterisation of leached chalcopyrite surfaces using scanning electron microscopy [5,6]. This phenomenon has

^{*} Corresponding author.

E-mail address: omid.marzoughi@queensu.ca (O. Marzoughi).

been recognized as one of the major reasons for the slow oxidative leaching kinetics of sulfide concentrates in aqueous systems. Additionally, in the ensuing gold leaching process, the gold recovery is reduced and the cyanide consumption is increased as the sulfur coats the surface of the gold [7,8]. Several techniques have been employed to remove this sulfur during the leaching process including using organic solvents [9,10], flotation [11,12], sulfur distillation and condensation [13], solid sorbents [14,15,16,17] and vacuum distillation [18,19]. When compared with each other, these procedures have various inherent characteristic advantages and disadvantages. However, the use of solid sorbents for the adsorption of sulfur is of considerable interest, due to the simple design, the cost effectiveness and the recyclability [20,21]. Consequently, in the present research, adsorption by a novel solid sorbent, Lanxess Lewatit® AF 5, was investigated for removing the elemental sulfur.

Carbonaceous-based catalysts have a high carbon content, a large specific surface area and substantial internal porosity [22,23,24]. The adsorbent properties including pore size distribution, surface area and functional groups, play key roles in the adsorption process. Under leaching conditions, catalyst properties such as solubility, size, acid solubility and electron distribution are the significant factors which influence adsorption as well as the operating variables such as temperature and solution pH. These parameters can affect the affinity between the sulfur and the adsorbent and/or have an effect on the adsorbent/adsorbate interactions [25]. Materials such as AF 5 have been utilized to adsorb various elements in a number of different processes [26,27,28,29,30,31]. Sulfur adsorption by activated carbon has previously been investigated by various researchers and the results showed that the adsorption process depends primarily on the characteristics of the adsorbent, the properties of the sulfur and the operating conditions [32,33,34]. Currently, activated carbons are used as one of the sorbents in enargite and pyrite leaching processes to remove sulfur and also to increase the reaction rates [35,36].

While activated carbon has the advantage of a high adsorption capacity, which makes it favorable for adsorption process, the costs of production are high, and the activated carbon can be both expensive and difficult to regenerate. Consequently, researchers have developed alternative catalysts. Currently, synthetic resin catalysts are one of the practical alternatives for adsorption processes. One critical advantage of the new resins is the relatively strong binding forces encountered in the adsorption processes in comparison to the weaker binding forces on activated carbon [37,38]. Adsorption capacity, porosity, adsorption rate and adsorbent cost are the most important factors utilized for the selection of novel adsorbents for the removal of sulfur from the leach residue. In addition, the adsorbent recovery and regeneration processes are important from both the economic and environmental perspectives [20,21].

Recently, a new type of carbon adsorbent, AF 5 has been developed and applied in the sulfide leaching processes. This adsorbent possesses significant advantages over other activated carbons [14,15,20,21,35,36]. It has been demonstrated that AF 5 has a much greater adsorption capacity and a higher adsorption rate than the other activated carbons. Microporous carbonaceous adsorbents, such as AF 5, are porous resins with both high surface area and high chemical resistance. This high adsorption capacity is one of the critical properties of the AF 5 which makes it an efficient catalyst in various processes. The application of AF 5 during the chalcopyrite leaching process has demonstrated that it can remove all the elemental sulfur from the leach solution [20,21]. The sulfur loaded AF 5 can be regenerated and reused in the leaching process. Another attractive property of AF 5 is its superior mechanical properties, leading to negligible AF 5 attrition losses during the leaching and regeneration processes.

Numerous techniques have been investigated for the adsorption of different metals and compounds from liquid samples produced during solvent extraction, chemical precipitation, coagulation, ultrafiltration, reverse osmosis, electrolytic processes, ion exchange, and adsorption on solid substrates [39,40,41,42,43,44,45]. The investigation of adsorption processes by both theoretical and experimental techniques is critical for a complete understanding of the behavior of the adsorbent. Although the majority of the previous research has focused on experimental studies, mathematical modeling is a useful technique and can be used to provide an improved interpretation of the adsorption processes involved in sulfur removal during the leaching process. The adsorption isotherms can be determined using the Langmuir and the Freundlich models. Also, the adsorption kinetics at the solid/solution interface can be modelled using the pseudo-first order (PFO) and the pseudo-second order (PSO) models. One of the critical properties of an adsorbent is the adsorption capacity, which is the percentage of elemental sulfur that can be adsorbed by the AF 5 per gram of adsorbate. The particle size distribution, pore size and distribution, cation exchange capacity, surface functional groups, specific surface area, temperature and pH are the most important variables which can control the adsorption capacity. The maximum adsorption capacities can be calculated using the adsorption isotherm plot.

1.1. Theoretical considerations

1.1.1. Adsorption isotherms

The adsorption isotherm describes the equilibrium relationship between the amount of sulfur on the AF 5 (or residue) and in the solution. Knowledge of this equilibrium data is crucial for designing the adsorption process. The adsorption capacities can be defined according to the following equation:

$$q_t = \frac{(C_0 - C_t)V}{M} \quad (2)$$

where q_t is the adsorption capacity in mg/g, C_0 and C_t are the initial concentrations of elemental sulfur and the concentration at time t , respectively; V is the volume of the solution (L) and m is the mass of the resin particles (g). In the present research, the sulfur content was reported in terms of mass and thus the equation could also be represented as follows:

$$q_t = \frac{m_0 - m_t}{M} \quad (3)$$

where m_0 is the initial mass of elemental sulfur and m_t is the elemental sulfur mass at time t .

The adsorption isotherm describes the equilibrium relationship between the quantity of the adsorbed material (elemental sulfur) and the sulfur concentration on the AF 5 at a constant temperature [46]. Data can be obtained which can be used to determine the maximum adsorption capacity and the maximum adsorption strength. This information can be used for predicting the optimum experimental conditions. Data for the adsorption isotherms were obtained using the batch method with different amounts of the AF 5 in the acidic Albion leaching process at different temperatures.

1.1.2. Langmuir isotherm

The Langmuir model is based on the monolayer adsorption of sulfur on the surface of the AF 5. It is assumed that there is no interaction between the adsorbed elemental sulfur molecules and the neighbouring adsorption sites and also assumes equivalent energies of monolayer sorption onto the AF 5 surface [47]. The Langmuir isotherm model is normally stated as follows:

$$\frac{C_e}{C_{ads}} = \frac{1}{q_b} + \frac{C_e}{q_m} \quad (4)$$

where C_e is the equilibrium concentration of elemental sulfur (mg/L), C_{ads} is the amount of adsorbed elemental sulfur per gram at equilibrium, q_b (L/mg) and q_m (mg/g) are the Langmuir constants at a given temperature and are related to the adsorption capacity and the energy of adsorption, respectively.

The linearized form of the equation describing this model is as follows:

$$q_e = \frac{q_m b C_e}{1 + b C_e} \quad (5)$$

where q_e is the mass of elemental sulfur on the AF 5 after adsorption (mg/g), b is the adsorption coefficient, which is related to the affinity of the binding sites (L/mg). The sorption parameters, b and q_m can be obtained from the slope and intercept, respectively, of a plot of $1/q_e$ versus $1/C_e$. A dimensionless constant or separation factor (R_L) can be defined as follows:

$$R_L = \frac{1}{1 + b C_o} \quad (6)$$

where R_L describes the favourability of the adsorption process where $0 < R_L < 1$ is favorable, $R_L = 0$ is irreversible and $R_L > 1$ is unfavorable [48].

1.1.3. Freundlich isotherm

The Freundlich empirical model is employed to explain non-ideal adsorption processes that take place on heterogeneous surfaces with active sites with various energies and is based on multilayer adsorption at equilibrium. Additionally, this model assumes that physio-chemical sorption can occur. The non-linearized Freundlich isotherm is described as follows:

$$q_e = K_f C_e^{1/n} \quad n > 1 \quad (7)$$

The Freundlich isotherm model can be represented in linear form as follows:

$$\text{Log } q_e = \text{Log } K_f + \frac{1}{n} \text{Log } C_e \quad (8)$$

where K_f is the Freundlich isotherm coefficient, n is related to adsorption intensity and surface heterogeneity, C_e is the equilibrium concentration of elemental sulfur (mg/L), q_e is the mass of elemental sulfur adsorbed at equilibrium (mg/g). The two terms K_f and n can be obtained from a plot of $\log q_e$ versus $\log C_e$ as they correspond to the slope and intercept, respectively. If the value of $1/n$ is between 0 and 1, the reaction is favorable, while for $1/n = 0$ the reaction would be irreversible and for $1/n > 1$ adsorption would be unfavorable [49].

1.1.4. Adsorption kinetics

The mechanisms of elemental sulfur sorption onto AF 5 can be investigated by determining the adsorption kinetics. This kinetic information is a crucial parameter that can be utilized for the design of adsorption systems and also to analyse the adsorption performance of the resin. Additionally, it can be used to minimise the residence time of the sorbate at the solid-solution interface. Different kinetic models have been applied to the experimental data in order to provide more information about the adsorption mechanisms. In this research, the adsorption kinetics and the rate constants of elemental sulfur adsorption onto AF 5 were studied by using various kinetic models, such as the pseudo-first order (PFO) and the pseudo-second order (PSO) models. As the correlation coefficients (R^2) were too low for the various other models, they were not considered. The PFO kinetic model describes the relationship between the number of available sites and the rate of filling of the sites on the AF 5. On the other hand, the PSO model relates the time to the adsorption capacity of the adsorbent. Both adsorption kinetic models are based on equilibrium adsorption as follows:

$$\ln(q_e - q_t) = \ln q_e - (k_1 t) \quad (9)$$

$$t/q_t = 1/k_2q_c^2 + t/q_c \quad (10)$$

where q_e and q_t represent the mass of elemental sulfur adsorbed onto AF 5 (mg/g) at equilibrium and at time t (mins), respectively; k_1 (min^{-1}) and k_2 (mg/(g min)) are the rate constants of adsorption. The value of k_1 is obtained as the slope of a linear plot of $\ln(q_e - q_t)$ versus time. The experimental value of q_e can be contrasted with the value obtained from the PFO model and if the difference is large, then the reaction cannot be classified as first-order. The value of k_2 was determined by plotting t/q_t against time and using the slope and intercept to arrive at a linear equation.

1.1.5. Adsorption thermodynamics

The thermodynamic properties for the adsorption of elemental sulfur on AF 5 were determined in order to further understand the adsorption process. These values such as change in free energy (ΔG°), change in enthalpy (ΔH°), and change in entropy (ΔS°) provide information about the adsorbent applicability, the nature of the adsorption process and the spontaneity of the adsorption. The thermodynamic parameters for sulfur adsorption by AF 5 were obtained from the following equations 11 and 12 [50,51,52]:

$$\Delta G_{ads}^\circ = -RT \ln K_L \quad (11)$$

$$\ln K_L = -\frac{\Delta H_{ads}^\circ}{RT} + \frac{\Delta S_{ads}^\circ}{R} \quad (12)$$

where K_L is the Langmuir isotherm constant, which is related to the affinity of sulfur for the binding sites (L/mg), T is the temperature

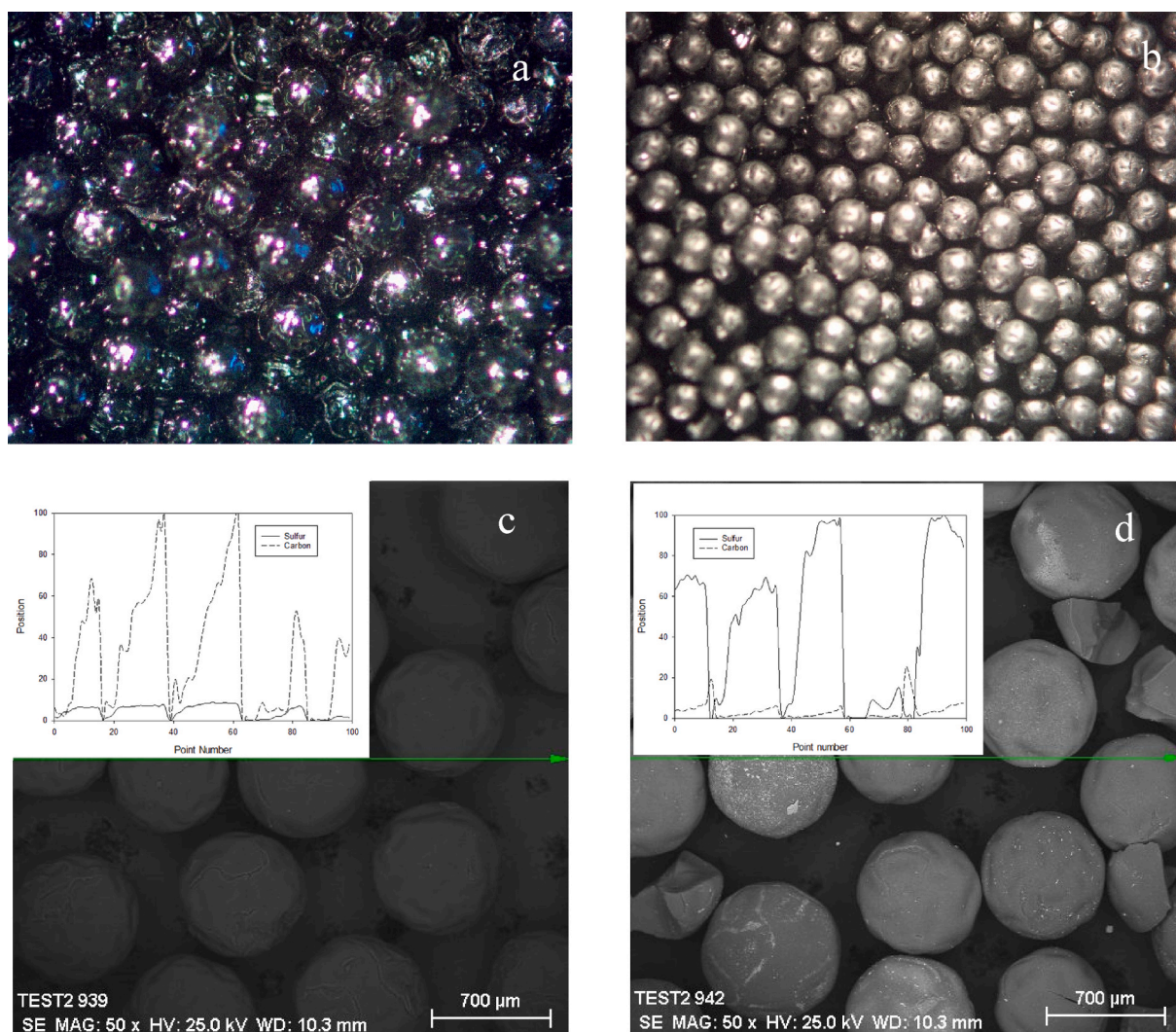


Fig. 1. Stereo optical micrographs of (a) as-received AF 5 and (b) S-AF 5 EDS(line scan) analysis of (c) as-received AF 5. (d) S-AF 5.

(K) and R is the gas constant (8.314 J/(mol K)).

Recently, a new experimental leaching process has been reported regarding the use of AF 5 for the removal of sulfur from the acidic Albion leaching of chalcopyrite [20,21]. The main objective of the present work was to investigate the sulfur adsorption mechanisms on AF 5 in the acidic Albion leaching process. Consequently, equilibrium experiments have been performed to study both elemental sulfur adsorption and the mechanism of sulfur removal. Adsorption isotherms for elemental sulfur on the AF 5 as a function of temperature, concentrate to resin ratio and mixing rate were investigated. Using this information, empirical equations were derived to describe the adsorption process. Furthermore, both the process kinetics and the thermodynamics could be evaluated for sulfur adsorption in the acidic Albion leaching process for chalcopyrite.

2. Experimental

2.1. Raw materials

The catalyst employed in this research was AF 5 which was produced from a synthetic polymer. It has a very strong mechanical strength and a narrow bead size distribution. The AF 5 resin has a spherical shape with a surface area of 1154 (m²/g) and a size range of 0.3–0.8 mm [53]. Prior to starting each experiment, the AF 5 was placed in stirred distilled water for 15 min. Then the catalyst was dried in the oven at 100 °C for 48 h until a constant weight of AF 5 was achieved.

The as-received AF 5 contained 98% carbon, about 1.2% moisture and less than 1% sulfur. Stereo optical micrographs and SEM micrographs of the fresh and post-leached AF 5 are compared in Fig. 1 (a–d). Fresh AF 5 had a wrinkled surface with visible pores. These pores and the irregular surface likely contributed to the total surface area and acted as active sites for the adsorption of elemental sulfur. After leaching, the sulfur-loaded AF-5 (S-AF 5) beads had a regular and smooth surface as the pores were filled with elemental sulfur. The SEM image of the S-AF 5 shows that the sulfur content increased significantly as the AF 5 adsorbed the elemental sulfur in the leaching process.

The leaching test work was performed on a chalcopyrite concentrate with a P₈₀ of 33.8 μm and required very little sample preparation prior to the acidic Albion leaching. The concentrate was analyzed through the use of QEMSCAN and ICP and the results are shown in Tables 1 and 2. The main minerals were chalcopyrite and pyrite and their concentrations were calculated to be 50.2% and 36.7%, respectively. The head assay showed that the concentrate contained 23.0% copper, 35.0% sulfur and 32.5% iron. Pentahydrate ferric sulfate (Acros Organics, 97.0%), hexahydrate ferric chloride (Acros Organics, 97.0%) and pentahydrate cupric sulfate (Fisher chemicals, 98.0%) were used in the leaching process to generate the required sulfate species in the leach solution.

2.2. Acidic albion leaching process adsorption experiments procedure

The detailed procedure for the acidic Albion leaching test has been published elsewhere [20,21] and only a summary is provided here. For determination of elemental sulfur adsorption by AF 5, a series of experiments were conducted in 2 L reactors inside a glass-kettle batch reactor. A thermocouple and reflux condenser were used for controlling the temperature and to prevent excessive evaporation, respectively. A sample of 100 g of chalcopyrite in 1 L of 100 g/L sulfuric acid solution with the addition of FeSO₄·7H₂O (7 g/L), Fe₂(SO₄)₃·5H₂O (3 g/L), and CuSO₄·5H₂O (1.5 g/L) and 25 g of fresh AF 5 were mixed and oxygen was sparged into the system at the rate of 1.5 L/min. The 25 g/L sulfuric acid solution with the addition of the appropriate amount of the sulfates was prepared and added to the system in order to maintain the pH value around 1. The acidic Albion leaching experiments were performed at 95 °C and for 48 h to ensure that equilibrium was attained. After the leaching test, the S-AF 5 was separated from the slurry by screening and then the leach slurry was pressure filtered. Both the S-AF 5 and the slurry were rinsed with DI water and dried in the vacuum oven at 40 °C for 3 days and then the sulfur concentration of the S-AF 5 and the residue were measured using an Eltra CS-2000 Carbon–Sulfur analyzer.

The elemental sulfur content of the residue was calculated using two different methods. In the first method, the weight percentages of elemental sulfur and sulfide were quantified based on a method using TGA analysis. Since elemental sulfur evaporates at

Table 1
Mineralogy of chalcopyrite concentrate.

| Component | Wt% |
|------------------------|---------------|
| Chalcopyrite | 50.2 |
| Bornite | 4.4 |
| Covellite + Chalcocite | 3.9 |
| Tet-Ten-En | 0.6 |
| Fe-Sulphide | 36.7 |
| Other Sulphides | 0.2 |
| Quartz | 1.3 |
| Feldspar | 0.4 |
| Mica | 1.3 |
| Fe–Ti-Oxide | 0.4 |
| Other Silicates | 0.3 |
| Other | 0.3 |
| <i>Total</i> | <i>100.00</i> |

Table 2
Chemical analysis of the chalcopyrite concentrate.

| Component | Copper | Iron | Calcium | Sulfur | Arsenic |
|-----------|--------|------|---------|--------|---------|
| wt% | 23.0 | 32.5 | 0.3 | 35.0 | 0.3 |

200–350 °C, then the sulfur speciation in the residue can be determined. At temperatures of 170–450 °C, the elemental sulfur was completely removed. The additional weight loss which began at approximately 480 °C and continued until 700 °C was attributed to sulfide. In the second method, the residue was mixed with toluene at 90 °C and the elemental sulfur was dissolved in the organic solvent. Also, the total sulfur content of the residue was determined using a C–S analyser both before and after treatment with toluene and the elemental sulfur content was calculated by comparison of the two numbers.

2.3. Studies of adsorption isotherm

The batch adsorption experiments were performed in the acidic Albion leaching system in 0.25 L 3-headed flasks where 2.5 g of the fresh AF 5 and the predetermined amount of sulfate leach solution (as described above) were added to the system. Subsequently, the flask was placed on a temperature-controlled magnetic stirrer (Arex digital, VELP Scientifica), which could be stirred at various rates. The pH of the solution was continuously measured by a pH meter (Fisher Scientific XL600 accumet) and maintained at 1. The isotherm studies were performed with different initial concentrations of chalcopyrite. In this way, the concentrate to AF 5 ratio was varied as follows: 1:1, 2:1, 4:1, 6:1 and 8:1. The isotherm data were fitted to two models (Langmuir and Freundlich).

2.4. Adsorption kinetics and thermodynamics

The elemental sulfur adsorption kinetics and thermodynamic were investigated at four temperatures ranging from 65 °C to 95 °C using batch conditions at a concentrate to AF 5 ratio of 4:1 for a 48 h contact time. During the leach tests several mL of solution including AF 5 was sampled using a syringe at different time intervals. The samples were then centrifuged at 5000 rpm for 5 min and filtered through a screen and then 0.45 µm syringe filters to separate the insoluble particles from the liquid phases. The operating parameters for each test are outlined in Table 3.

3. Results and discussion

The results of the solid analysis during the investigation are summarized in Table 4. The amount of elemental sulfur in the residue is given as well as the adsorbed sulfur on the AF 5 for each test.

3.1. Effect of AF 5 resin

The effect of the AF 5 carbon-based resin on the behavior of the elemental sulfur in the acidic Albion leaching process was investigated. In Fig. 2 the behavior of the elemental sulfur both with and without AF 5 for concentrate to catalyst ratios of 4:1 and 8:1 were compared after 48 h of leaching at 95 °C. It can be seen that after the leaching test, with a concentrate to AF 5 ratio of 4:1, all the elemental sulfur was adsorbed onto the surface of the AF 5 and there was no elemental sulfur remaining on the residue. However, for the concentrate to AF 5 catalyst ratio of 8:1 only about 55% of the elemental sulfur was captured on the catalyst and the remainder precipitated with the residue. For a concentrate to AF 5 ratio of 4:1, the rate of adsorption with respect to contact time on the surface of the AF 5 initially increased rapidly and this was followed by a gradual decrease until equilibrium was reached. The rapid increase was

Table 3
Operating parameters for the oxidation tests.

| Test | Volume (L) | Temperature (°C) | Concentrate to AF 5 ratio | Agitation speed(rpm) |
|------|------------|------------------|---------------------------|----------------------|
| C 1 | 1 | 95 | No AF 5 | 800 |
| C 2 | 1 | 95 | 4:1 | 800 |
| C 3 | 1 | 95 | 8:1 | 800 |
| C 4 | 0.1 | 95 | 4:1 | 600 |
| C 5 | 0.1 | 95 | 4:1 | 800 |
| C 6 | 0.1 | 95 | 4:1 | 1000 |
| C 7 | 0.1 | 65 | 4:1 | 800 |
| C 8 | 0.1 | 75 | 4:1 | 800 |
| C 9 | 0.1 | 85 | 4:1 | 800 |
| C 10 | 0.1 | 95 | 4:1 | 800 |
| C 11 | 0.1 | 95 | 1:1 | 800 |
| C 12 | 0.1 | 95 | 2:1 | 800 |
| C 13 | 0.1 | 95 | 4:1 | 800 |
| C 14 | 0.1 | 95 | 6:1 | 800 |
| C 15 | 0.1 | 95 | 8:1 | 800 |

Table 4
Solid sample analysis results from the oxidation tests.

| Test | Elemental sulfur in residue (%) | Elemental sulfur on AF 5 (%) |
|------|---------------------------------|------------------------------|
| C 1 | 100 | No AF 5 |
| C 2 | 0 | 100 |
| C 3 | 47 | 53 |
| C 4 | 0 | 100 |
| C 5 | 0 | 100 |
| C 6 | 0 | 100 |
| C 7 | 0 | 100 |
| C 8 | 0 | 100 |
| C 9 | 0 | 100 |
| C 10 | 0 | 100 |
| C 11 | 0 | 100 |
| C 12 | 0 | 100 |
| C 13 | 0 | 100 |
| C 14 | 28 | 72 |
| C 15 | 48 | 52 |

When using AF 5 during leaching, the copper and iron recoveries were above 95% and 80%, respectively after 48 h and AF 5 have not affected the base metals recovery in the leaching process [18,19].

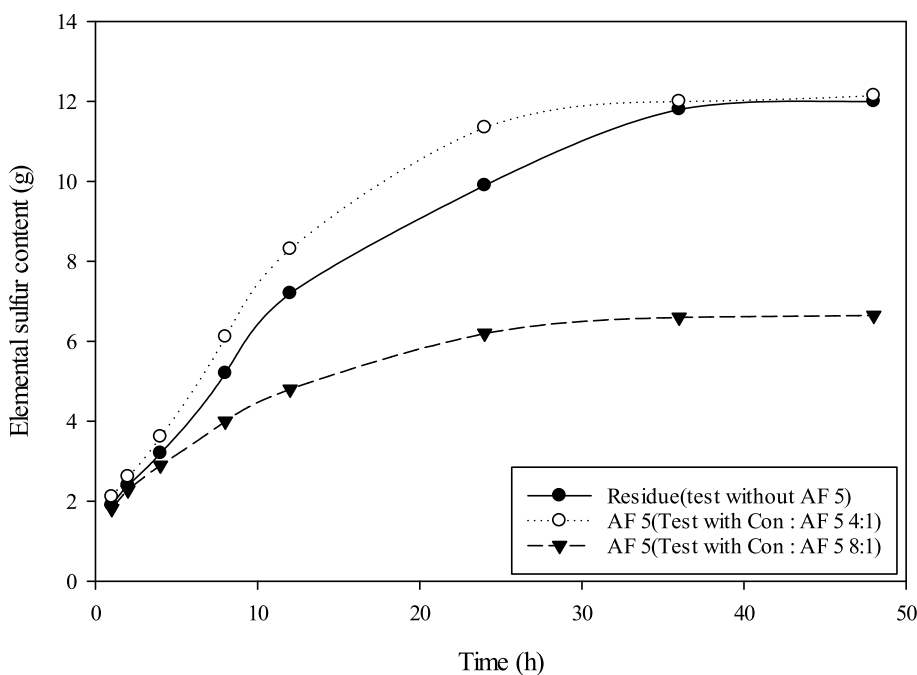


Fig. 2. Comparison of the elemental sulfur content of the leach residue(in the absence of AF 5) and sulfur loaded AF 5 at different concentrate: AF 5 ratios.

attributed to the large surface area and the large number of vacant sites on the fresh AF 5. As the plateau was approached, the surface pores of the AF 5 began to fill with elemental sulfur. In the absence of AF 5, the initial rate of rise of the sulfur content of the residue was again rapid, but it was slower than for the test with AF 5. Furthermore, although the rate of rise of the sulfur content of the residue decreased at extended times it remained higher than the test with AF 5. These results showed that the equilibrium amount of sulfur which was converted to elemental sulfur during leaching was slightly higher (12 g elemental sulfur without AF 5 and 12.2 g in the presence of AF 5) in the presence of AF 5 at the concentrate to AF 5 ratio of 4:1. The amount of elemental sulfur after 48 h increased from 12.0 g in the absence of AF 5–12.15 g with AF 5.

3.2. Effect of agitation speed

The adsorption batch experiments were carried out with different agitation speeds varying from 600 to 1000 rpm, in order to study the influence of the agitation speed on the adsorption. These experiments were conducted at 95 °C for 48 h for a 4 to 1 ratio of concentrate to AF 5. The optimum agitation speed for adsorption depends on both the configuration of the reactor and the slurry

properties such as viscosity, density and volume. The effect of the agitation rate on the adsorption process is shown in Fig. 3. As can be seen, the mixing rate did not have a significant effect on the sulfur adsorption rate nor the equilibrium sulfur adsorption. The sulfur adsorption increased only slightly with increasing mixing rate from 454 mg/g at 600 rpm to about 474 mg/g at 1000 rpm. The relatively small influence of the mixing rate can be attributed to the minimization of the film boundary layer surrounding the particles for all stirring rates. Without a film boundary layer, the external film transfer coefficients increased and, hence, also the adsorption capacity [54]. The stirring rate of 800 rpm was chosen as the control agitation speed for all the subsequent experiments.

3.3. Effect of temperature

The effect of temperature on the uptake of elemental sulfur by AF 5 was investigated at different temperatures while the concentrate to AF 5 ratio and the mixing rate were fixed at 4 and 800 rpm, respectively. As shown in Fig. 4, the elemental sulfur adsorption onto the AF 5 particles decreased with increasing temperature, demonstrating the exothermic nature of the adsorption process. The sulfur adsorption of AF 5 after 48 h was 474 mg/g at 65 °C and increased to 402 mg/g at 95 °C. Thus, the affinity of the elemental sulfur in the solution for the AF-5 decreased with increasing temperature. It can be seen that the majority of the sulfur adsorption on the AF 5 in the temperature range of 65–95 °C was completed within 25–30 h. For instance, after 12, 24, and 36 h of adsorption, the adsorbed elemental sulfur percentages at 65 °C were 68%, 93% and 98% respectively.

3.4. Effect of concentrate to AF 5 mass ratio

The mass of the AF 5 in the leaching tests is an important variable that influences the adsorption of elemental sulfur. The effect of concentrate to AF 5 ratio on the elemental sulfur adsorption on the AF 5 using various masses of concentrate is shown in Fig. 5. The results showed that initially, the rate of sulfur adsorption on AF 5 increased with the mass of chalcopyrite. It can be seen that for concentrate to AF 5 ratios of less than 4:1, the sulfur adsorption tended to increase with increasing amount of concentrate (and hence sulfur), from 120 mg/g to about 474 mg/g. However, the tests at higher concentrate to catalyst ratios exhibited similar sulfur adsorptions after 48 h. Increasing the amount of AF 5 relative to the concentrate, enhanced the sulfur removal from the leaching process since it provided more surface area for adsorption. However, the amount of sulfur adsorbed per AF 5 unit mass decreased. This was mainly due to the saturation of the adsorption sites.

3.5. Adsorption isotherms

The Langmuir and the Freundlich isotherm models were used to study the sulfur adsorption on the AF 5 (eq. (5) and eq. (8)). The maximum adsorption capacity corresponds to the saturation of the sites on the AF 5 and can be obtained from the plateau region of the plot. The Langmuir model defines monolayer sorption on homogenous surfaces while the Freundlich model assumes that the adsorption occurs on a heterogeneous surface [55,56].

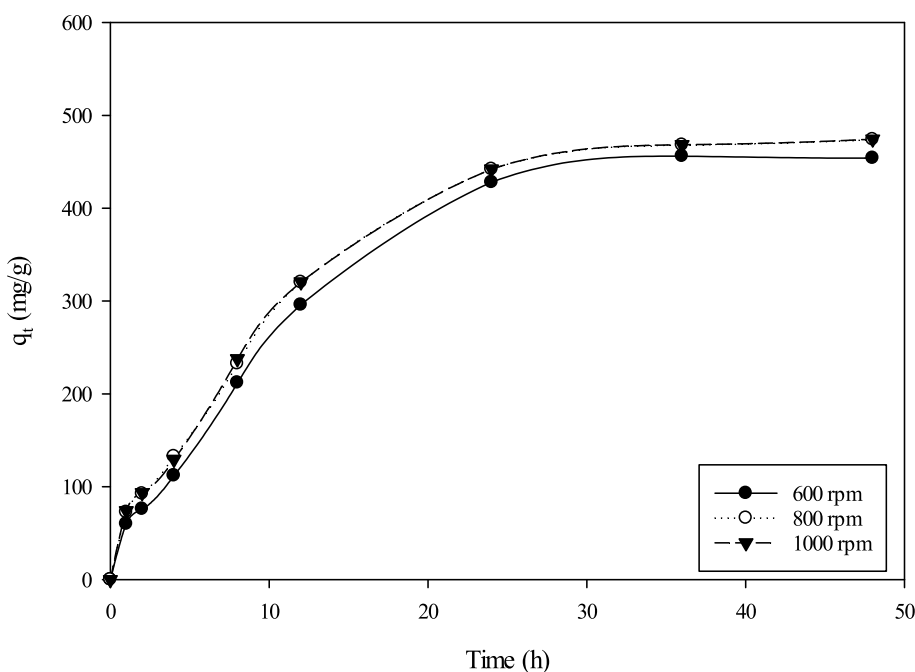


Fig. 3. Effect of mixing rate on sulfur adsorption onto AF 5.

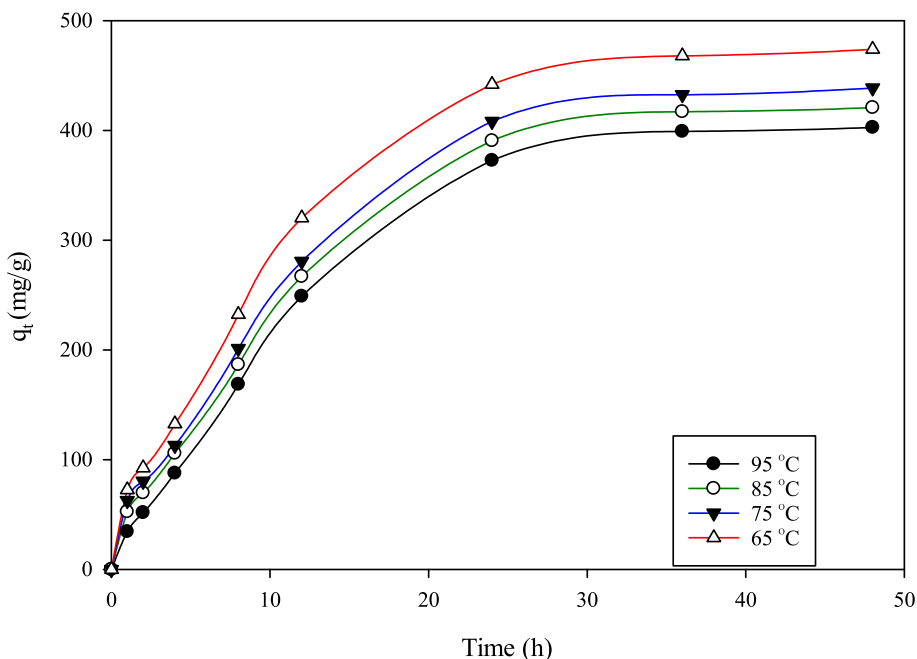


Fig. 4. Effect of temperature on sulfur adsorption on AF 5 after 48 h.

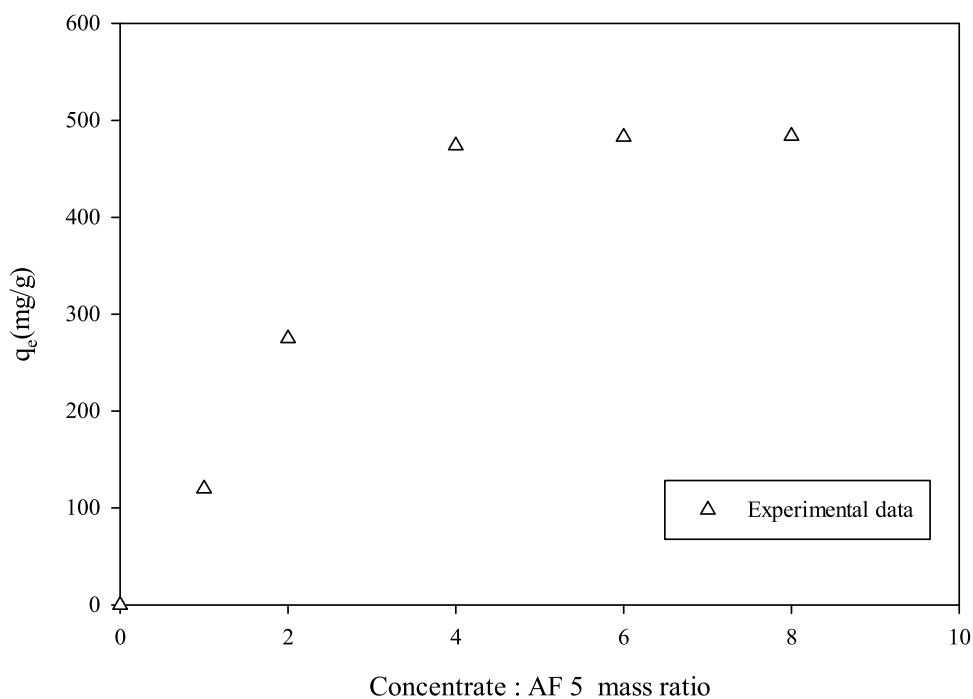


Fig. 5. The effect of concentrate to AF 5 mass ratio on sulfur adsorption onto AF 5 after 48 h.

Based on the experimental data, R^2 values were obtained for the sorption of sulfur on the AF 5 for both isotherm models. Fig. 6 (a,b) shows plots of both the Langmuir adsorption and the Freundlich adsorption. The results showed that the Langmuir isotherm model ($R^2 = 0.99$) had a significantly better fit to the data than the Freundlich isotherm model ($R^2 = 0.88$). These results again indicate that the mechanism of sulfur adsorption on the AF 5 involves monolayer sorption. The Langmuir isotherm model was used to predict the adsorption capacity and then these values were compared to the experimental adsorption capacity. The comparison showed that the adsorption capacity value which was obtained from the Langmuir isotherm was close to the experimental value. The maximum

adsorption capacity was obtained, and the value was $Q_m = 488$ mg/g. This value corresponds to the saturation of a fixed number of identical surface sites in the Langmuir model. Thus, temperature should not have an effect on the maximum capacity [48,57,58,59,60,61]. However, the bonding between the adsorbate and any potential adsorption sites became weaker at higher temperatures. This would indicate that the adsorption process was physical, and this can be contrasted with the opposing behavior in chemisorption.

Table 5 shows the isotherm parameters for elemental sulfur adsorption onto the surface of the AF 5. The dimensionless constant R_L and the Langmuir isotherm constant K_L were calculated by utilizing the model equations for the leaching system and the values were 0.002 and 0.1 L/mg, respectively. A value of R_L less than 1 indicates that sulfur adsorption onto the AF 5 was a favorable process. These values would be consistent with monolayer sorption where the elemental sulfur would be adsorbed on different AF 5 sites with no transmigration of the elemental sulfur on the surface [54].

Based on the above analysis, AF 5 has a relatively high adsorption capacity for sulfur onto AF 5 in comparison to other sorbents for sulfur removal during chalcopyrite leaching [8]. Thus, it can be stated that using AF 5 to remove elemental sulfur from the acidic Albion leaching process has a significant advantage over other methods and thus is an attractive alternative.

3.6. Adsorption kinetics modeling

The plots of both the PFO and the PSO equations (eq. (9) and eq. (10)) are shown at various temperatures in Fig. 7(a and b) and both plots exhibit a linear relationship. The PFO model fits the experimental data well for different temperatures, as the R^2 values are close to one (>0.98) and thus the theoretical model and the experimental data are in good agreement. The PSO model had lower R^2 values and a poorer fit and thus there were significant differences between the theoretical model and the experimental data.

Table 6 shows the kinetic parameters for the adsorption of the elemental sulfur onto the AF 5. The kinetic parameters show that both the amount of adsorption and the rate of adsorption increased with increasing temperature. Therefore, the adsorption process is more efficient at higher temperatures. For both models, the small value of K indicates that the adsorption process is relatively slow. The R^2 values for the sulfur adsorption kinetics were slightly higher for the PFO model than for the PSO model. As shown in Table 4, the K_1 value increased from 4.8×10^{-7} (/min) to 5.6×10^{-7} (/min) as the temperature increased from 65 °C to 95 °C. The values of the adsorption capacity (q_e) which were derived from the slope of the plot in Fig. 7 increased from 409 mg/g to 475 mg/g when the temperature increased from 65 °C to 95 °C, respectively. These values are close to the experimental values of 474 mg/g at 95 °C and this demonstrates that the PFO model is in good agreement with the experiments.

The PSO kinetic model did exhibit a good fit to the test data for all temperatures as the correlation coefficients (R^2) were only slightly lower than the corresponding PFO values. For this model it is assumed that each elemental sulfur atom is adsorbed onto two adsorption sites of the carbonaceous adsorber. The value of the rate constant increased with increasing temperature. At 65 °C the rate constant was 1.5×10^{-6} g/mg min and this increased to 2.7×10^{-6} g/mg min at 95 °C. The corresponding q_e values from the PSO model were 588 mg/g and 592 mg/g at 65 °C and 95 °C, respectively and these were not close to the experimental values of 402 mg/g and 474 mg/g, respectively. This demonstrates that the PSO model does not provide a good fit to the experimental data for sulfur adsorption by the AF 5.

3.7. Thermodynamic parameters

The values of $\ln K_L$ are plotted against $1/T$ in Fig. 8 and the entropy and enthalpy values were calculated from the intercept and the slope, respectively. The calculated values for the change in Gibbs free energy, change in enthalpy and change in entropy are presented in Table 7. The ΔH_{ads}^0 value was -9.1 (kJ/mol) and this indicates that the adsorption process of the elemental sulfur onto the AF 5 is exothermic. Also, the magnitude of this enthalpy change, which is in the range of 2.1–20.9 kJ/mol indicates that physical adsorption is more favorable. The small negative value of ΔS_{ads}^0 of -0.1 (kJ/mol·K) suggests that the adsorption of the elemental sulfur onto the AF 5 results in a slightly more ordered structure. The changes in the standard Gibbs free energy were calculated over the temperature range of 65 °C–95 °C. The negative ΔG_{ads}^0 values over the whole temperature range demonstrate that elemental sulfur adsorption onto AF 5 is spontaneous in nature. Additionally, the ΔG_{ads}^0 values are in the range of 0 to -20 kJ/mol and this again suggests that the adsorption is a physical process [50,57].

4. Conclusions

The adsorption isotherms, the kinetics and the thermodynamics for the adsorption of elemental sulfur on Lewatit® AF 5 resin have been determined for the acidic Albion leaching process. It was determined that this carbonaceous resin is an efficient adsorbent for elemental sulfur. The results showed that the AF 5 can adsorb 100% of the sulfur at 95 °C. The experimental results showed that the sorption process was affected by both the temperature and the concentrate to AF 5 ratio. Agitation speed did not have a significant effect. The kinetic study demonstrated that the rate of adsorption is high, and the adsorption process can be well described by the pseudo first-order model. The adsorption isotherm data were fitted to the Langmuir and the Freundlich models. The equilibrium isotherm results showed that the adsorption process could be best represented by the Langmuir model with a maximum adsorption capacity of 488 mg/g. The calculated separation factor, R_L , was greater than 1, which demonstrated that AF 5 was an efficient adsorbent. Based on the thermodynamic studies, the negative values of ΔG_{ads}^0 and ΔH_{ads}^0 demonstrated that the removal of elemental sulfur by the AF 5 was thermodynamically feasible, exothermic, and spontaneous. The slightly negative value of ΔS_{ads}^0 showed that there was a small decrease in randomness due to the adsorption of the elemental sulfur on the AF 5. The magnitudes of the ΔG_{ads}^0 and ΔH_{ads}^0 values suggested that the adsorption of the sulfur onto the AF 5 is a physical process.

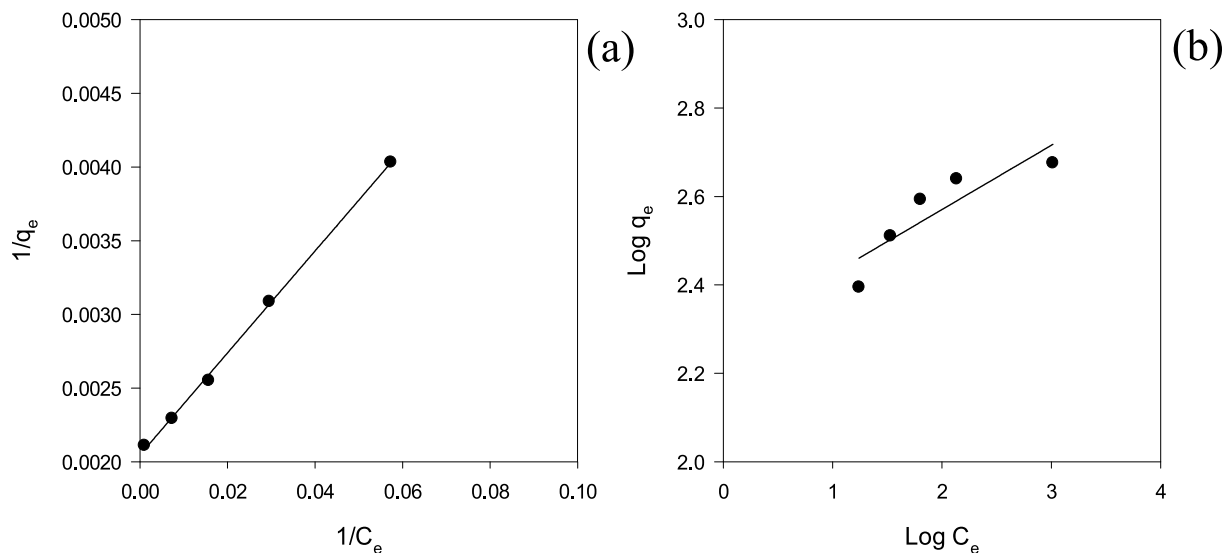


Fig. 6. Adsorption isotherm plots (a) Langmuir adsorption isotherm (b) Freundlich adsorption isotherm.

Table 5

Adsorption isotherm parameters for the adsorption of elemental sulfur onto AF 5.

| Adsorption Isotherm Model | Parameter | AF 5 |
|---------------------------|--------------|-------|
| Langmuir Isotherm | Q_m (mg/g) | 488.2 |
| | K_L (L/mg) | 0.1 |
| | R_L | 0.002 |
| | R^2 | 0.99 |
| Freundlich Isotherm | k_f (mg/g) | 190.6 |
| | $1/n$ | 6.9 |
| | n | 0.2 |
| | R^2 | 0.88 |

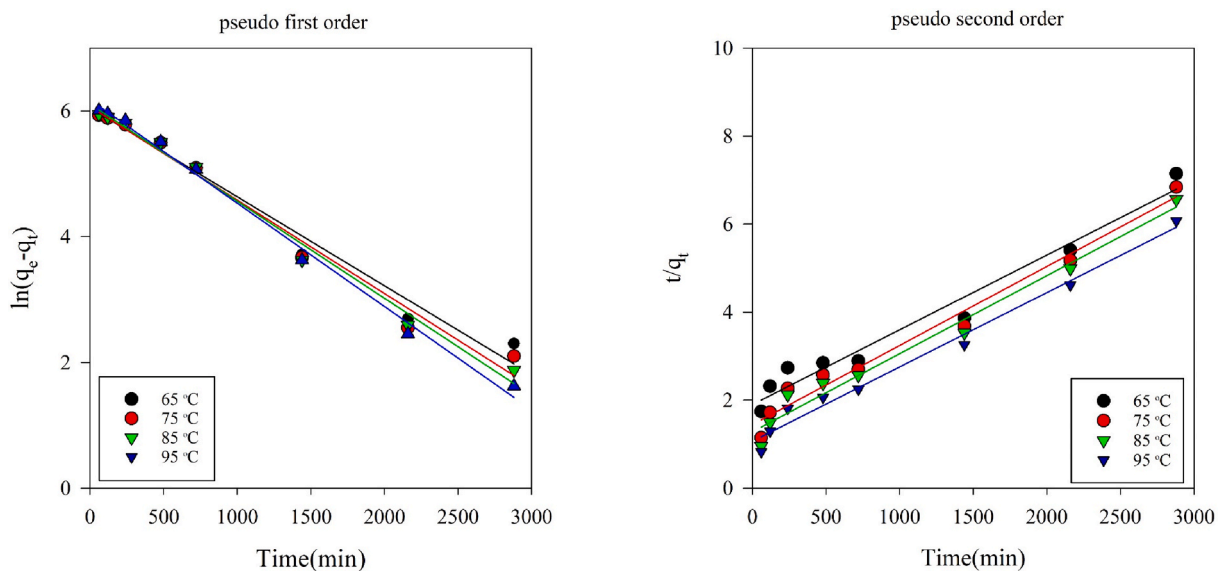


Fig. 7. Kinetic model plots for elemental sulfur adsorption onto AF 5: (a) pseudo first order and (b) pseudo second order.

Table 6
Parameters for the PFO and PSO kinetic models.

| Kinetic Model | Parameter | 65 °C | 75 °C | 85 °C | 95 °C |
|---------------------|------------------|----------------------|----------------------|----------------------|----------------------|
| Pseudo-first-order | K_1 (/min) | 4.8×10^{-7} | 5.1×10^{-7} | 5.3×10^{-7} | 5.6×10^{-7} |
| | q_e (mg/g) | 408.7 | 425.9 | 443.9 | 475.3 |
| | R^2 | 0.99 | 0.98 | 0.99 | 0.99 |
| Pseudo-second-order | K_2 (g/mg.min) | 1.5×10^{-6} | 2.2×10^{-6} | 2.5×10^{-6} | 2.7×10^{-6} |
| | q_e (mg/g) | 588.4 | 556.4 | 563.5 | 591.9 |
| | R^2 | 0.966 | 0.979 | 0.975 | 0.976 |

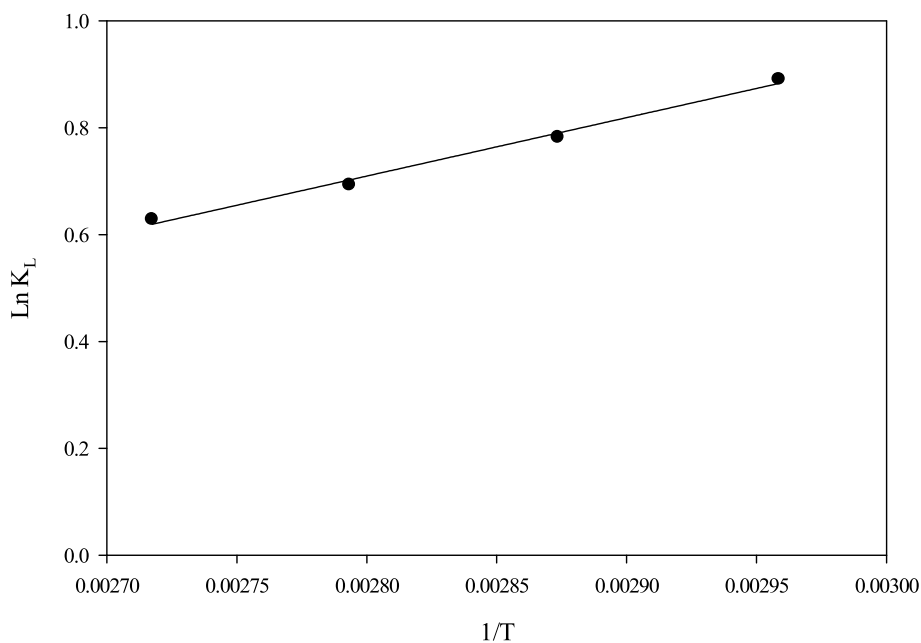


Fig. 8. Plot of $1/T$ versus $\ln K_L$ for sulfur adsorption on AF 5.

Table 7
Thermodynamic parameters for the adsorption of elemental sulfur onto AF 5.

| T (°C) | ΔG_{ads}° (kJ/mol) | ΔH_{ads}° (kJ/mol) | ΔS_{ads}° (kJ/mol·K) |
|--------|-----------------------------------|-----------------------------------|-------------------------------------|
| 65 | -2.5 | -9.1 | -0.1 |
| 75 | -2.2 | | |
| 85 | -2.1 | | |
| 95 | -1.9 | | |

Author contribution statement

Omid Marzoughi: Conceived and designed the experiments; Performed the experiments; Analyzed and interpreted the data; Wrote the paper.

Chris Pickles, Ahmad Ghahreman: Analyzed and interpreted the data; Contributed reagents, materials, analysis tools or data; Wrote the paper.

Funding statement

Ahmad Ghahreman was supported by Natural Sciences and Engineering Research Council of Canada [CRDPJ 531189 - 18].

Data availability statement

Data will be made available on request.

Declaration of interest's statement

The authors declare no competing interests.

References

- [1] M.M. Antonijević, G.D. Bogdanović, Investigation of the leaching of chalcopyritic ore in acidic solutions, *Hydrometallurgy* 73 (2004) 245–256, <https://doi.org/10.1016/j.hydromet.2003.11.003>.
- [2] D.A. Clark, P.R. Norris, Oxidation of mineral sulphides by thermophilic microorganisms, *Miner. Eng.* 9 (1996) 1119–1125, [https://doi.org/10.1016/0892-6875\(96\)00106-9](https://doi.org/10.1016/0892-6875(96)00106-9).
- [3] M. Hourn, D.W. Turner, *COMMERCIALISATION OF THE ALBION PROCESS, ALTA, Perth, Australia, 2012*, p. 19.
- [4] P. Voigt, M. Hourn, D. Mallah, D. Turner, Commissioning and Ramp-Up of the Albion Process at the GPM Gold Project, *MetPlant*, 2015, p. 14.
- [5] D. Dreisinger, Case study flowsheets: copper–gold concentrate treatment, in: M.D. Adams, B.A. Wills (Eds.), *Developments in Mineral Processing*, Elsevier, 2005, pp. 825–848, [https://doi.org/10.1016/S0167-4528\(05\)15033-9](https://doi.org/10.1016/S0167-4528(05)15033-9).
- [6] M.E. Chalkley, M.J. Collins, E. Ozberk, *The Behaviour of Sulphur in the Sherritt Zinc Pressure Leach Process, World Zinc '93.*, 1993, pp. 325–331.
- [7] J.E. Halfyard, K. Hawboldt, Separation of elemental sulfur from hydrometallurgical residue: a review, *Hydrometallurgy* 109 (2011) 80–89, <https://doi.org/10.1016/j.hydromet.2011.05.012>.
- [8] E. Jorjani, A. Ghahreman, Challenges with elemental sulfur removal during the leaching of copper and zinc sulfides, and from the residues; a review, *Hydrometallurgy* 171 (2017) 333–343, <https://doi.org/10.1016/j.hydromet.2017.06.011>.
- [9] T. Havlík, R. Kammel, Leaching of chalcopyrite with acidified ferric chloride and carbon tetrachloride addition, *Miner. Eng.* 8 (1995) 1125–1134, [https://doi.org/10.1016/0892-6875\(95\)00077-4](https://doi.org/10.1016/0892-6875(95)00077-4).
- [10] P. Peng, H. Xie, L. Lu, Leaching of a sphalerite concentrate with H₂SO₄–HNO₃ solutions in the presence of C₂Cl₄, *Hydrometallurgy* 80 (2005) 265–271, <https://doi.org/10.1016/j.hydromet.2005.08.004>.
- [11] S. Lin, R. Liu, W. Li, W. Sun, Y. Hu, Clean desulfurization of sulfur-rich tungsten concentrates by reverse flotation, *J. Clean. Prod.* 244 (2020), 118876, <https://doi.org/10.1016/j.jclepro.2019.118876>.
- [12] G. Liu, K. Jiang, B. Zhang, Z. Dong, F. Zhang, F. Wang, T. Jiang, B. Xu, Selective flotation of elemental sulfur from pressure acid leaching residue of zinc sulfide, *Minerals* 11 (2021) 89, <https://doi.org/10.3390/min11010089>.
- [13] Y. c/o, D.M.C.L. Watanabe, T. c/o, D.M.C.L. Fujita, K. c/o, D.M.C.L. Saruta, Method of Recovering Sulfur from Leach Residues of Sulfidic Ore Processing Using Distillation and Condensation, EP1179605B1, 2004. <https://patents.google.com/patent/EP1179605B1/pt>. (Accessed 24 August 2020). accessed.
- [14] D.H. Cowan, F.G. Jahromi, A. Ghahreman, A parameters study of the novel atmospheric pyrite oxidation process with Lewatit® AF 5 catalyst, *Hydrometallurgy* 183 (2019) 87–97, <https://doi.org/10.1016/j.hydromet.2018.11.014>.
- [15] F.G. Jahromi, D.H. Cowan, A. Ghahreman, Lanxess Lewatit® AF 5 and activated carbon catalysis of enargite leaching in chloride media; a parameters study, *Hydrometallurgy* 174 (2017) 184–194, <https://doi.org/10.1016/j.hydromet.2017.10.012>.
- [16] R. Ozola, A. Krauklis, M. Leitiets, J. Burlakovs, I. Vircava, L. Ansone-Bertina, A. Bhatnagar, M. Klavins, FeOOH-modified clay sorbents for arsenic removal from aqueous solutions, *Environ. Technol. Innovat.* 13 (2019) 364–372, <https://doi.org/10.1016/j.eti.2016.06.003>.
- [17] A. Krauklis, R. Ozola, J. Burlakovs, K. Rugele, K. Kirillov, A. Trubaca-Boginska, K. Rubenis, V. Stepanova, M. Klavins, FeOOH and Mn₈O₁₀Cl₃ modified zeolites for As(V) removal in aqueous medium, *J. Appl. Chem. Biotechnol.* 92 (2017) 1948–1960, <https://doi.org/10.1002/jctb.5283>.
- [18] H. Li, X. Wu, M. Wang, J. Wang, S. Wu, X. Yao, L. Li, Separation of elemental sulfur from zinc concentrate direct leaching residue by vacuum distillation, *Separ. Purif. Technol.* 138 (2014) 41–46, <https://doi.org/10.1016/j.seppur.2014.09.036>.
- [19] H. Li, X. Yao, M. Wang, S. Wu, W. Ma, W. Wei, L. Li, Recovery of elemental sulfur from zinc concentrate direct leaching residue using atmospheric distillation: a pilot-scale experimental study, *J. Air Waste Manag. Assoc.* 64 (2014) 95–103.
- [20] O. Marzoughi, L. Li, C. Pickles, A. Ghahreman, Thermal treatment of Lanxess Lewatit® AF 5 resin used in the atmospheric chalcopyrite leaching process: regeneration and sulfur recovery, *Chemosphere* 295 (2022), 133890, <https://doi.org/10.1016/j.chemosphere.2022.133890>.
- [21] O. Marzoughi, L. Li, C. Pickles, A. Ghahreman, Regeneration and sulfur recovery of Lanxess Lewatit AF 5 catalyst from the acidic Albion leaching process using toluene and tetrachloroethylene as organic solvents, *J. Ind. Eng. Chem.* 107 (2022) 291–301, <https://doi.org/10.1016/j.jiec.2021.11.055>.
- [22] M. Barczak, K. Michalak-Zwierzy, K. Gdula, K. Tyszczyk-Rotko, R. Dobrowolski, Ordered mesoporous carbons as effective sorbents for removal of heavy metal ions, *Microporous Mesoporous Mater.* 211 (2015) 162–173, <https://doi.org/10.1016/j.micromeso.2015.03.010>.
- [23] K. Pyrzyńska, Carbon nanostructures for separation, preconcentration and speciation of metal ions, *TrAC, Trends Anal. Chem.* 29 (2010) 718–727, <https://doi.org/10.1016/j.trac.2010.03.013>.
- [24] T. Naseem, F. Bibi, S. Arif, M. Waseem, S. Haq, M.N. Azra, T. Liblik, I. Zekker, Adsorption and kinetics studies of Cr (VI) by graphene oxide and reduced graphene oxide-zinc oxide nanocomposite, *Molecules* 27 (2022) 7152, <https://doi.org/10.3390/molecules27217152>.
- [25] Q.-S. Liu, T. Zheng, P. Wang, J.-P. Jiang, N. Li, Adsorption isotherm, kinetic and mechanism studies of some substituted phenols on activated carbon fibers, *Chem. Eng. J.* 157 (2010) 348–356, <https://doi.org/10.1016/j.cej.2009.11.013>.
- [26] G. Chakrapani, P.L. Mahanta, D.S.R. Murty, B. Gomathy, Preconcentration of traces of gold, silver and palladium on activated carbon and its determination in geological samples by flame AAS after wet ashing, *Talanta* 53 (2001) 1139–1147, [https://doi.org/10.1016/S0039-9140\(00\)00601-9](https://doi.org/10.1016/S0039-9140(00)00601-9).
- [27] K. Jankowski, A. Jackowska, P. Łukasiak, Determination of precious metals in geological samples by continuous powder introduction microwave induced plasma atomic emission spectrometry after preconcentration on activated carbon, *Anal. Chim. Acta* 540 (2005) 197–205, <https://doi.org/10.1016/j.aca.2004.09.012>.
- [28] O.N. Kononova, A.G. Kholmogorov, N.V. Danilenko, S.V. Kachin, Y.S. Kononov, Zh.V. Dmitrieva, Sorption of gold and silver on carbon adsorbents from thiocyanate solutions, *Carbon* 43 (2005) 17–22, <https://doi.org/10.1016/j.carbon.2004.08.021>.
- [29] R. Chand, T. Watari, K. Inoue, H. Kawakita, H.N. Luitel, D. Parajuli, T. Torikai, M. Yada, Selective adsorption of precious metals from hydrochloric acid solutions using porous carbon prepared from barley straw and rice husk, *Miner. Eng.* 22 (2009) 1277–1282, <https://doi.org/10.1016/j.mineng.2009.07.007>.
- [30] C. Moreno-Castilla, Adsorption of organic molecules from aqueous solutions on carbon materials, *Carbon* 42 (2004) 83–94, <https://doi.org/10.1016/j.carbon.2003.09.022>.
- [31] Z.R. Yue, W. Jiang, L. Wang, H. Toghiani, S.D. Gardner, C.U. Pittman, Adsorption of precious metal ions onto electrochemically oxidized carbon fibers, *Carbon* 37 (1999) 1607–1618, [https://doi.org/10.1016/S0008-6223\(99\)00041-X](https://doi.org/10.1016/S0008-6223(99)00041-X).
- [32] J. Li, L. Zhang, T. Wang, J. Chang, Z. Song, C. Ma, Study on sulfur migration in activated carbon adsorption-desorption cycle: effect of alkali/alkaline earth metals, *J. Environ. Sci.* 99 (2021) 119–129, <https://doi.org/10.1016/j.jes.2020.06.009>.
- [33] A. Bagreev, S. Bashkova, T.J. Bandoz, Adsorption of SO₂ on activated carbons: the effect of nitrogen functionality and pore sizes, *Langmuir* 18 (2002) 1257–1264.
- [34] F. Sun, J. Gao, X. Liu, X. Tang, S. Wu, A systematic investigation of SO₂ removal dynamics by coal-based activated cokes: the synergic enhancement effect of hierarchical pore configuration and gas components, *Appl. Surf. Sci.* 357 (2015) 1895, <https://doi.org/10.1016/j.apsusc.2015.09.118>. –1901.
- [35] D.H. Cowan, F.G. Jahromi, A. Ghahreman, Atmospheric oxidation of pyrite with a novel catalyst and ultra-high elemental sulphur yield, *Hydrometallurgy* 173 (2017) 156–169, <https://doi.org/10.1016/j.hydromet.2017.07.003>.
- [36] F.G. Jahromi, G. Alviai-Hein, D.H. Cowan, A. Ghahreman, The kinetics of enargite dissolution in chloride media in the presence of activated carbon and AF 5 catalysts, *Miner. Eng.* 143 (2019), 106013, <https://doi.org/10.1016/j.mineng.2019.106013>.
- [37] S.-H. Lin, R.-S. Juang, Adsorption of phenol and its derivatives from water using synthetic resins and low-cost natural adsorbents: a review, *J. Environ. Manag.* 90 (2009) 1336–1349, <https://doi.org/10.1016/j.jenvman.2008.09.003>.

- [38] Y. Lu, Y. Liu, B. Xia, W. Zuo, Phenol oxidation by combined cavitation water jet and hydrogen peroxide, *Chin. J. Chem. Eng.* 20 (2012) 760–767, [https://doi.org/10.1016/S1004-9541\(11\)60246-2](https://doi.org/10.1016/S1004-9541(11)60246-2).
- [39] MdR. Awwal, Novel nanocomposite materials for efficient and selective mercury ions capturing from wastewater, *Chem. Eng. J.* 307 (2017) 456–465, <https://doi.org/10.1016/j.cej.2016.08.108>.
- [40] MdR. Awwal, MdM. Hasan, J. Iqbal, MdA. Islam, A. Islam, S. Khandaker, A.M. Asiri, M.M. Rahman, Ligand based sustainable composite material for sensitive nickel(II) capturing in aqueous media, *J. Environ. Chem. Eng.* 8 (2020), 103591, <https://doi.org/10.1016/j.jece.2019.103591>.
- [41] MdR. Awwal, Solid phase sensitive palladium(II) ions detection and recovery using ligand based efficient conjugate nanomaterials, *Chem. Eng. J.* 300 (2016) 264–272, <https://doi.org/10.1016/j.cej.2016.04.071>.
- [42] MdR. Awwal, Assessing of lead(III) capturing from contaminated wastewater using ligand doped conjugate adsorbent, *Chem. Eng. J.* 289 (2016) 65–73, <https://doi.org/10.1016/j.cej.2015.12.078>.
- [43] MdR. Awwal, A. Islam, M.M. Hasan, M.M. Rahman, A.M. Asiri, M.A. Khaleque, M. Chanmiya Sheikh, Introducing an alternate conjugated material for enhanced lead(II) capturing from wastewater, *J. Clean. Prod.* 224 (2019) 920–929, <https://doi.org/10.1016/j.jclepro.2019.03.241>.
- [44] H. Md Munjur, MdN. Hasan, MdR. Awwal, MdM. Islam, M.A. Shenashen, J. Iqbal, Biodegradable natural carbohydrate polymeric sustainable adsorbents for efficient toxic dye removal from wastewater, *J. Mol. Liq.* 319 (2020), 114356, <https://doi.org/10.1016/j.molliq.2020.114356>.
- [45] K.T. Kubra, MdS. Salman, MdN. Hasan, A. Islam, MdM. Hasan, MdR. Awwal, Utilizing an alternative composite material for effective copper(II) ion capturing from wastewater, *J. Mol. Liq.* 336 (2021), 116325, <https://doi.org/10.1016/j.molliq.2021.116325>.
- [46] I.D. Mall, V.C. Srivastava, N.K. Agarwal, Removal of Orange-G and Methyl Violet dyes by adsorption onto bagasse fly ash—kinetic study and equilibrium isotherm analyses, *Dyes Pigments* 69 (2006) 210–223.
- [47] F.M. Morel, J.G. Hering, *Principles and Applications of Aquatic Chemistry*, John Wiley & Sons, 1993.
- [48] E. Malkoc, Y. Nuhoglu, Investigations of nickel(II) removal from aqueous solutions using tea factory waste, *J. Hazard Mater.* 127 (2005) 120–128, <https://doi.org/10.1016/j.jhazmat.2005.06.030>.
- [49] M.M. Rahman, M. Adil, A.M. Yusof, Y.B. Kamaruzzaman, R.H. Ansary, Removal of heavy metal ions with acid activated carbons derived from oil palm and coconut shells, *Materials* 7 (2014) 3634–3650, <https://doi.org/10.3390/ma7053634>.
- [50] A. Christian, N.B. Eligwe, Adsorption thermodynamics and kinetics of mercury (II), cadmium (II) and lead (II) on lignite, *Chem. Eng. Technol.* 22 (1999) 45–49.
- [51] A. Özer, D. Özer, A. Özer, The adsorption of copper(II) ions on to dehydrated wheat bran (DWB): determination of the equilibrium and thermodynamic parameters, *Process Biochem.* 39 (2004) 2183–2191, <https://doi.org/10.1016/j.procbio.2003.11.008>.
- [52] İ. Uzun, F. Güzel, Kinetics and thermodynamics of the adsorption of some dyestuffs and p-nitrophenol by chitosan and MCM-chitosan from aqueous solution, *J. Colloid Interface Sci.* 274 (2004) 398–412, <https://doi.org/10.1016/j.jcis.2004.02.022>.
- [53] Ghahreman Jahromi, Effect of surface modification with different acids on the functional groups of AF 5 catalyst and its catalytic effect on the atmospheric leaching of enargite, *Colloid. Interf.* 3 (2019) 45, <https://doi.org/10.3390/colloids3020045>.
- [54] A. Wołowicz, Z. Hubicki, Carbon-based adsorbent resin Lewatit AF 5 applicability in metal ion recovery, *Microporous Mesoporous Mater.* 224 (2016) 400–414, <https://doi.org/10.1016/j.micromeso.2015.12.051>.
- [55] B.H. Hameed, I.A.W. Tan, A.L. Ahmad, Adsorption isotherm, kinetic modeling and mechanism of 2, 4, 6-trichlorophenol on coconut husk-based activated carbon, *Chem. Eng. J.* 144 (2008) 235–244.
- [56] Y. Liu, Y.-J. Liu, Biosorption isotherms, kinetics and thermodynamics, *Separ. Purif. Technol.* 61 (2008) 229–242.
- [57] A.Y. Dursun, A comparative study on determination of the equilibrium, kinetic and thermodynamic parameters of biosorption of copper(II) and lead(II) ions onto pretreated *Aspergillus Niger*, *Biochem. Eng. J.* 28 (2006) 187–195, <https://doi.org/10.1016/j.bej.2005.11.003>.
- [58] X. Wang, Y. Qin, Z. Li, Biosorption of zinc from aqueous solutions by rice bran: kinetics and equilibrium studies, *Separ. Sci. Technol.* 41 (2006) 747–756, <https://doi.org/10.1080/01496390500527951>.
- [59] M. Dundar, C. Nuhoglu, Y. Nuhoglu, Biosorption of Cu(II) ions onto the litter of natural trembling poplar forest, *J. Hazard Mater.* 151 (2008) 86–95, <https://doi.org/10.1016/j.jhazmat.2007.05.055>.
- [60] V. Padmavathy, Biosorption of nickel(II) ions by baker's yeast: kinetic, thermodynamic and desorption studies, *Bioresour. Technol.* 99 (2008) 3100–3109, <https://doi.org/10.1016/j.biortech.2007.05.070>.
- [61] R. Djeribi, O. Hamdaoui, Sorption of copper(II) from aqueous solutions by cedar sawdust and crushed brick, *Desalination* 225 (2008) 95–112, <https://doi.org/10.1016/j.desal.2007.04.091>.